Aalborg Universitet

An Iterative Transfer Matrix Computation Method for Propagation Graphs in Multi-Room Environments

Adeogun, Ramoni; Bharti, Ayush; Pedersen, Troels

An Iterative Transfer Matrix Computation Method for Propagation Graphs in Multi-Room Environments

Ramoni Adeogun, Ayush Bharti and Troels Pedersen

Abstract—**This paper presents a reduced complexity method for computing the transfer matrix of wireless channels in complex indoor environments with a large number of rooms using propagation graphs. Multi-room indoor environments can be represented in a vector signal flow graph with rooms in the complex structure as nodes and propagation between rooms as branches. We propose an iterative procedure to compute the transfer matrix of such complex graphs. The state vector for each node in the graph is iteratively computed until convergence. The state vector for the room(s) with the receiver is then used to compute the transfer function. We show via simulations that the proposed approach closely approximates the original model at much reduced complexity.**

Index Terms—**Multi-room indoor environment, propagation graph, channel model, signal flow graph, complexity**

I. INTRODUCTION

PROPAGATION graphs (PGs) provide a flexible structure for modelling multlink channels with account for multiple scattering. PGs describe the channel as a directed graph with the transmitters, receivers and scatterers as vertices and interactions between vertices as time-invariant transfer functions. Based on the graph description, closed-form expressions for the channel transfer function is given in [1].

The PG model has been applied to different scenarios including: millimetre wave [2], high speed railway [3]–[6], indoor to outdoor [7], and polarized [8] channel. Hybrid models combining the PG with other modelling frameworks have also been studied in [9]–[12]. However, as a result of a matrix inversion in the closed form expression, the computation cost increases with increasing number of scatterers, thereby making it unattractive for large environments such as large buildings, indoor offices and even outdoor environments where the number of scatterers is large.

In [13], a reduced complexity equivalent of the PG model for multi-room indoor environments comprising of a number of adjacent rooms is presented. The PG for the environment is transformed into a vector signal flow graph (VSFG) with the rooms as nodes. A closed form expression is then derived for the channel transfer matrix by applying a matrix equivalent of Mason's rule to the VSFG. Although this method yields same prediction as the original PG model, it requires that the number

of scatterers in all rooms be equal, which is not realistic in general environments.

In this letter, we propose a more general method for computing the transfer matrix without any restriction on the number of scatterers per room. The method involves iterative computation of the state matrices for each room in the building based on node equations obtained from the VSFG.

II. PROPAGATION GRAPH MODEL

Following [1], we consider a simple directed graph $\mathcal{G} = (\mathcal{V}, \mathcal{E})$ where vertex set $\mathcal{V} = \mathcal{V}_\text{t} \cup \mathcal{V}_\text{s} \cup \mathcal{V}_\text{r}$ is a union of three disjoint sets: a set of N_t transmitters, $\mathcal{V}_\text{t}$, a set of N_s scatterers, $\mathcal{V}_\text{s}$ and a set of N_r receivers, $\mathcal{V}_\text{r}$. Wave propagation between the vertices is modelled by edges in $\mathcal{E}$. An edge, $e = (v, w)$, exists if and only if a wave can propagate directly from v to w. The propagation graph exhibits a special structure; transmit vertices have no incoming edges; receive vertices have no outgoing edges; and there are no loops in the graph, i.e., no edge, $e = (w, w)$ is possible between the same vertex, w. It should however be noted that cycles may exist in the graph.

Wave propagation in the graph is defined by the actions of the scatterers and edges. A scatterer re-emits weighted version of the sum of signals arriving via the incoming edges to the outgoing edges. An edge $e = (v, w) \in \mathcal{E}$ transfers a signal from v to w according to its transfer function, $A_e(f)$, defined as

$$A_e(f) = \begin{cases} g_e(f) \exp(j2\pi f \tau_e + \phi_e); & e \in \mathcal{E} \\ 0; & e \notin \mathcal{E} \end{cases} \quad (1)$$

where $g_e(f)$, τ_e and ϕ_e are the gain, propagation delay and random phase of the edge, respectively. The edge transfer functions are collected into sub-matrices:

$$\mathbf{D}(f) \in \mathbb{C}^{N_\text{r} \times N_\text{t}} : \text{transmitters} \rightarrow \text{receivers}$$
$$\mathbf{T}(f) \in \mathbb{C}^{N_\text{s} \times N_\text{t}} : \text{transmitters} \rightarrow \text{scatterers}$$
$$\mathbf{R}(f) \in \mathbb{C}^{N_\text{r} \times N_\text{s}} : \text{scatterers} \rightarrow \text{receivers}$$
$$\mathbf{B}(f) \in \mathbb{C}^{N_\text{s} \times N_\text{s}} : \text{scatterers} \rightarrow \text{scatterers}.$$

Assuming that the channel is time-invariant, the received signal vector $\mathbf{Y}(f)$ reads

$$\mathbf{Y}(f) = \mathbf{H}(f)\mathbf{X}(f), \quad (2)$$

where $\mathbf{X}(f)$ is the transmitted signal vector and the transfer matrix, $\mathbf{H}(f) \in \mathbb{C}^{N_\text{r} \times N_\text{t}}$ of the propagation graph is expressed as

$$\mathbf{H}(f) = \mathbf{D}(f) + \mathbf{R}(f)[\mathbf{I} - \mathbf{B}(f)]^{-1}\mathbf{T}(f); \quad \rho(\mathbf{B}) < 1, \quad (3)$$
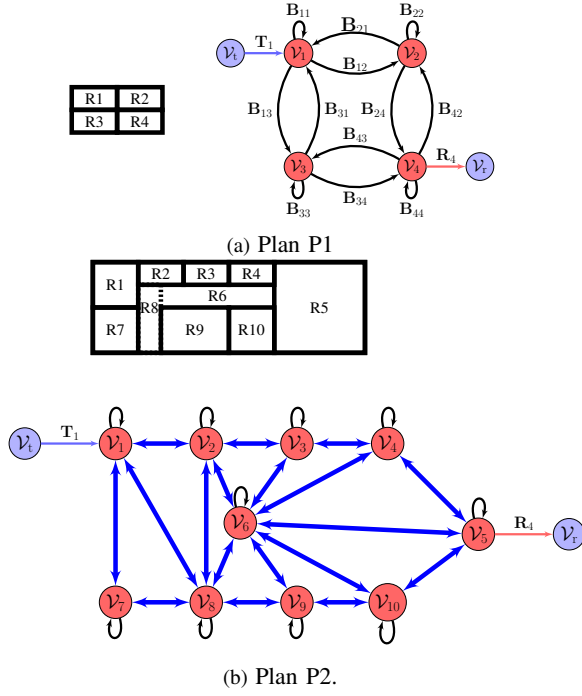
(a) Plan P1

(b) Plan P2.

Fig. 1: Illustration of VSFG representation. The dashed line in (b) denotes partition of an L-shaped corridor into two rooms.

where $\rho(\cdot)$ denotes the spectral radius. Evaluation of (3) at frequency, f, requires inversion of $N_{\mathrm{s}} \times N_{\mathrm{s}}$ matrix, which is an $\mathcal{O}(N_{\mathrm{s}}^3)$ operation.

III. REPRESENTATION OF MULTI-ROOM INDOOR ENVIRONMENTS AS VSFG

As shown in Fig. 1, the scatterers in the multi-room scenario are partitioned into N sub-sets, $\mathcal{V}_{\mathrm{s1}}, \mathcal{V}_{\mathrm{s2}} \ldots, \mathcal{V}_{\mathrm{sN}}$ according to rooms in the building. From this, a VSFG can be constructed by applying two rules:

1) Each scattering subset (i.e room), $\mathcal{V}_{\mathrm{sn}}$ is designated as a vertex with a loop corresponding to the interactions between scatterers within the room.
2) Inter-room propagation through walls are represented as edges between the nodes with each pair of neighbouring vertices having a forward and reverse going edge.

We define a state vector for each vertex in the VSFG as $\mathbf{S}_n \in \mathbb{C}^{N_{\mathrm{sn}} \times 1}; n = 1 \ldots, N$, where N_{sn} denotes the number of scatterers in room n. The state vector, $\mathbf{S}_n$, represents the signal at the output of scatterers in room n. The transmitted signal $\mathbf{X}$ corresponds to the state vector of the transmitting nodes. The signal in each room can be represented as (suppressing the frequency dependency for clarity)

$$\mathbf{S}_n = \mathbf{B}_{tn}\mathbf{X} + \mathbf{B}_{nn}\mathbf{S}_n + \sum_{m \in \mathcal{N}_n} \mathbf{B}_{mn}\mathbf{S}_m; \ n = 1, \ldots, N, \quad (4)$$

where

$$\mathbf{B}_{tn} = \begin{cases} \mathbf{T}_n & \text{if room } n \text{ has transmitter(s)} \\ \mathbf{0} & \text{if room } n \text{ has no transmitter(s),} \end{cases} \quad (5)$$

is the transfer matrix between the transmitters, $\mathcal{V}_{\mathrm{t}}$ and the scatterers in $\mathcal{V}_{\mathrm{sn}}$, $\mathbf{B}_{ij}$ is the transfer matrix between the scatterers

in the ith and jth rooms and $\mathcal{N}_n$ is the set of neighbours of node n. The state vector of the node corresponding to the receiver gives the channel transfer matrix as

$$\mathbf{H}_{nm} = \mathbf{D}_{nm} + \mathbf{R}_m\mathbf{S}_m, \quad (6)$$

where the direct transfer matrix $\mathbf{D}_{nm} \in \mathbb{C}^{N_{\mathrm{r}} \times N_{\mathrm{t}}}$, is only non-zero if $n = m$; $\mathbf{R}_m \in \mathbb{C}^{N_{\mathrm{r}} \times N_{\mathrm{sm}}}$ is the transfer matrix between the scatterers in $\mathcal{V}_{\mathrm{sm}}$ and the receivers, $\mathcal{V}_{\mathrm{r}}$.

We write the expression in (4) in the form:

$$\mathbf{S}_n = [\mathbf{I} - \mathbf{B}_{nn}]^{-1}(\mathbf{B}_{tn}\mathbf{X} + \sum_{m \in \mathcal{N}_n} \mathbf{B}_{mn}\mathbf{S}_m). \quad (7)$$

The factor $[\mathbf{I} - \mathbf{B}_{nn}]^{-1}$ can be expanded into an infinite geometric series of the intra-room scattering matrix, $\mathbf{B}_{nn}$, capturing the infinite reverberations within room n. For realistic buildings, the scatterers in a room are strongly connected to each other; less strongly linked to scatterers in neighbouring rooms, and not connected at all to scatterers in rooms further away. We exploit this structure to solve (4) by iterating over inter-room interactions only, rather than iteration over all interactions.

IV. ITERATIVE STATE VECTOR COMPUTATION METHOD

Starting with an initial state vector, $\mathbf{S}_n[0] = \mathbf{0}; n = 1, \ldots, N$, the state matrices for all rooms are iteratively updated until convergence via

$$\mathbf{S}_n[k] = [\mathbf{I} - \mathbf{B}_{nn}]^{-1}(\mathbf{B}_{tn}\mathbf{X} + \sum_{m \in \mathcal{N}_n} \mathbf{B}_{mn}\mathbf{S}_m[k-1]); \ k = 1, 2, \cdots \quad (8)$$

The matrix inversions in (8) can be computed prior to the iterative procedure.

Theorem 1. *Provided that $\rho(\mathbf{B}) < 1$, the convergence of the iterative equation in* (8) *is guaranteed.*

Proof. Let $\mathbf{S} = [\mathbf{S}_1^T \cdots \mathbf{S}_N^T]^T$. Then by (4),

$$\mathbf{S}[k] = \mathbf{T}\mathbf{X} + \mathbf{B}\mathbf{S}[k-1]. \quad (9)$$

The error, $\epsilon[k] = \mathbf{S}[k] - \mathbf{S}[k-1]$ is bounded as

$$||\epsilon[k]|| = ||\mathbf{B}\epsilon[k-1]||$$
$$\leq ||\mathbf{B}|| \cdot ||\epsilon[k-1]||. \quad (10)$$

Since $\rho(\mathbf{B}) < 1$, $||\epsilon[k]|| < ||\epsilon[k-1]||$ and hence $\epsilon[k] \to 0$ for $k \to \infty$, which completes the proof. $\square$

To evaluate the speed of convergence of (8), we define a metric, ξ_{norm}, as the change in the norm of the state vectors of the rooms normalized by the norm at the previous iteration and averaged over all frequency values. Thus,

$$\xi_{\mathrm{norm}}[k] = \frac{1}{Z} \sum_{z=1}^{Z} \frac{||\mathbf{S}[k,z] - \mathbf{S}[k-1,z]||}{||\mathbf{S}[k-1,z]||}, \quad (11)$$

where Z denotes the number of frequency samples. The algorithm is said to have converged when ξ_{norm} is less than or equal to a predefined threshold ξ_{conv}.

The proposed Iterative State vector Computation Method (ISCM) is stated in Algorithm 1.

Algorithm 1 Iterative State Vector Computation Method (ISCM)

Input: N; $\mathbf{B}_{nm}$; $n/m = 1, \ldots, N$; $\mathbf{T}$; $\mathbf{R}$; ξ_{conv}
1: Initialization: $\mathbf{S}_n[0] = \mathbf{0}$; $\forall n$; $k = 0$; $\xi_{\mathrm{norm}} = 1$
2: Compute $\mathbf{C}_{nn} = [\mathbf{I} - \mathbf{B}_{nn}]^{-1}$ and $\mathcal{N}_n$ for all N.
3: **while** $\xi_{\mathrm{norm}} > \xi_{\mathrm{conv}}$ **do**
4:    $k = k + 1$
5:    **for** $n = 1 : N$ **do**
6:      **if** transmitter is in room n **then**
7:        $\mathbf{S}_n[k] = \mathbf{C}_{nn}(\mathbf{B}_{tn}\mathbf{S}_t + \sum_{m \in \mathcal{N}_n} \mathbf{B}_{mn}\mathbf{S}_m[k-1])$
8:      **else**
9:        $\mathbf{S}_n[k] = \mathbf{C}_{nn}(\sum_{m \in \mathcal{N}_n} \mathbf{B}_{mn}\mathbf{S}_m[k-1])$
10:     **end**
11:    **end**
12:    Compute ξ_{norm} using (11)
13: **end**
14: Compute $\mathbf{H}(f)$ using (6)
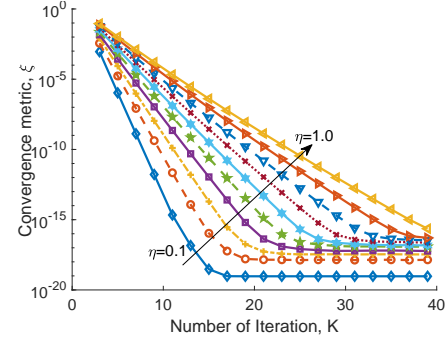**Output:** $\mathbf{H}(f)$

Fig. 2: Convergence metric, ξ_{norm} against number of iterations for structure P1 with wall penetration factor, η as parameter.
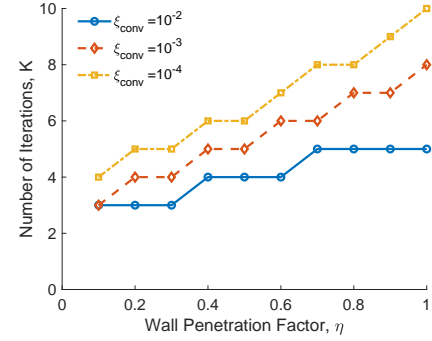

Fig. 3: Number of iterations against η for structure P1 with convergence threshold, ξ_{conv} as parameter.

V. COMPLEXITY ANALYSIS

Since the complexity of the PG using (3) and the ISCM is dominated by matrix multiplications and inversions, we count the number of such operations in the algorithms. For a general structure with N rooms and N_s scatterers per room, computing the transfer matrix at each frequency value using the PG model in (3) is dominated by the inversion of the $NN_s \times NN_s$ matrix, $\mathbf{B}$ and has time complexity, $\mathcal{O}(N^3 N_s^3)$. On the other hand, the dominant operation in the ISCM is inversion of the $N_s \times N_s$ matrix, $\mathbf{B}_{nn}$ for all N rooms. Therefore, the ISCM has time complexity, $\mathcal{O}(N N_s^3)$. Thus, as the number of rooms N increases, channel computation using the PG becomes more complex than with the ISCM.

VI. SIMULATION STUDY

We perform simulations to compare accuracy and time complexity of the ISCM with the original PG. We consider the two structures in Fig. 1, i.e., P1: a simple four-room building with transmitter(s) in room 1 and receiver(s) in room 4 and P2: a more complex 8-room building with transmitter in room 1 and receiver in reciever in room 5. As with the original model, the computation methods presented in this paper are generic in that they can be applied with general edge transfer functions. For our simulations, we utilize the edge transfer functions given in the example model in [1] and scale the transfer function of inter-room edges by a multiplicative wall penetration factor, $0 \leq \eta \leq 1$ to account for wall penetration losses. For simplicity, η is set equal for all walls in the simulations. This is however not a requirement of the method. Except where otherwise stated, the channel is generated following the procedures highlighted in [1] with the parameters in Table I. The scatterers are uniformly distributed within the volume of the rooms.

A. Algorithm Convergence

We utilize the convergence metric, ξ_{norm}, defined in (11). In Fig. 2, we plot the ξ_{norm} against number of iterations for P1. We observe that ξ_{norm} decays exponentially with fast
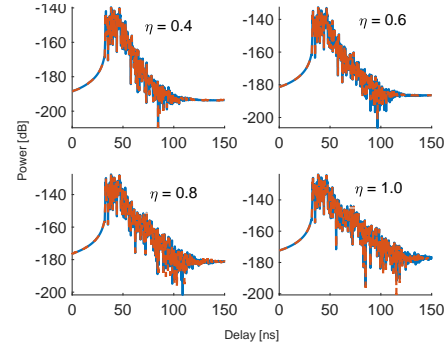

Fig. 4: PDP for a realization of the channel in P1 with $\xi_{\mathrm{conv}} = 10^{-3}$ and wall penetration factor, η as parameter.
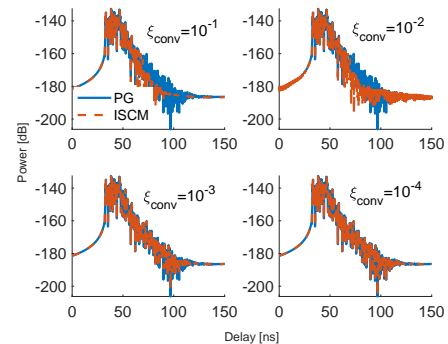

Fig. 5: PDP for a realization of the channel in P1 with different ξ_{conv} values.

TABLE I: Simulation Parameters.

Parameter	Value	Parameter	Value
Room sizes	$3 \times 4 \times 3\,\text{m}^3$	g	0.52
Freq. range	$58\,\text{GHz} - 62\,\text{GHz}$	P_{vis}	0.92
Numb. of samples	801	N_{s}	10
Transmitted signal	Rectangular pulse	ξ_{conv}	10^{-3}

TABLE II: Averaged total power, mean delay and RMS delay spread for Plan P1 with $\xi_{\text{conv}} = 10^{-3}$.

η	Total Power [dB]		Mean Delay [ns]		RMS DS [ns]	
	PG	**ISCM**	**PG**	**ISCM**	**PG**	**ISCM**
0.2	-143.60	-143.60	44.66	44.66	8.05	8.05
0.4	-131.75	-131.75	45.30	45.30	7.89	7.89
0.6	-124.66	-124.64	44.58	44.55	8.23	8.23
0.8	-119.37	-119.37	44.86	44.86	8.71	8.69
1.0	-115.62	-115.62	45.52	45.49	9.44	9.33

decay rates for all values of wall penetration factors considered indicating that convergence of the iterative computation procedure is guaranteed. With $\xi_{\text{conv}} = 10^{-2}$ (i.e., the norm of the the current state vector is equal to 99.9% of that of the previous state vector), the algorithm requires only about $K = 5$ iterations to converge. Fig. 3 shows that the number of iterations required for convergence increases with increasing wall penetration factor and also with decreasing value of ξ_{conv}.

B. Simulated Channel Comparison

We now compare the power delay profile (PDP) of the channel generated using both methods. Fig. 4 shows that, with $\xi_{\text{conv}} = 10^{-3}$, the PDP of P1 obtained from both methods are sufficiently close for all values of penetration factor considered. This indicates that a threshold value of $\xi_{\text{conv}} = 10^{-3}$ is sufficient to accurately generate the channel from the ISCM in this scenario. In Fig. 5, we notice a significant difference between the PDP from the PG and ISCM with threshold values of $\xi_{\text{conv}} = 10^{-1}$ and $\xi_{\text{conv}} = 10^{-2}$ and that PDP from both methods agree closely with $\xi_{\text{conv}} \geq 10^{-3}$. With $\xi_{\text{conv}} \geq 10^{-3}$, we observe in Tab. II that the averaged total power, mean delay and root mean square delay spread for both the PG and ISCM for P1 are nearly equal for all values of penetration factor considered.

Finally, Fig. 6 shows the PDP obtained from both methods for the more realistic 8 rooms structure with an L-shaped corridor with VSFG in Fig. 1b. We observe that a somewhat lower threshold, $\xi_{\text{conv}} \geq 10^{-4}$ is required to approximate the late part of the true PDP. The number of iterations to convergence are however seen to be similar to those in Fig. 3 for the simpler structure, P1.

C. Time Complexity

We now compare the computation time of ISCM with the PG via simulations. We set the number of iterations for the ISCM, $K = 5$. In Fig. 7, we observe that the PG has slightly lower time complexity than the ISCM at lower number of scatterers ($N_{\text{s}} \leq 90$) per room for P1. The computation time for the PG is also seen to grow much faster than that of the ISCM resulting in much lower computation time for the ISCM at $N_{\text{s}} \geq 100$. With $N_{\text{s}} = 180$, a computation time reduction of
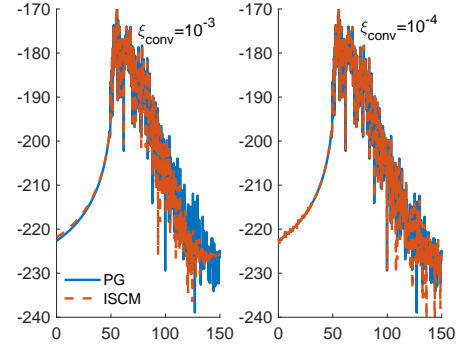

Fig. 6: PDP for P2 with 10 scatterers per room. The floor dimension of the rooms are $3 \times 4\,\text{m}^2$ for rooms 1,7,8 and 10, $3 \times 2\,\text{m}^2$ for rooms 3 and 4, $2 \times 2\,\text{m}^2$ for room 2, $6 \times 5\,\text{m}^2$ for room 5, $6 \times 2\,\text{m}^2$ for room 6 and $2 \times 6\,\text{m}^2$ for room 8. The building has a height of $3\,\text{m}$. Number of iterations to convergence is $K = 5(6)$ for $\xi_{\text{conv}} = 10^{-3}(10^{-4})$.
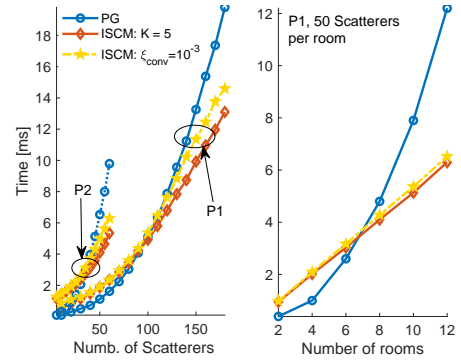

Fig. 7: Computation time per channel transfer function generation versus number of scatterers per room for both rooms and number of rooms with 50 scatterers per room for P1.

about $6\,\text{ms}(\approx 35\%)$ is obtained from using the ISCM. Similar trend is seen for P2 where the ISCM yields computation time saving of about $4.45\,\text{ms}(\approx 45.5\%)$ with 60 scatterers per room. Fig. 7 also shows that with increasing number of rooms, the computation time for the PG and ISCM exhibit cubic and linear growth, respectively. The PG requires slightly lower computation time than the ISCM with few rooms, but becomes more computationally intensive with further increase in N. Similar time complexity is seen in Fig. 7 for the ISCM with the convergence threshold, $\xi_{\text{conv}} = 10^{-3}$.

VII. CONCLUSION

The proposed iterative state vector computation method (ISCM) is able to reduce the complexity needed to compute channel transfer matrices in multi-room indoor environments based on a propagation graph (PG) model. The ISCM approximates the exact PG model to an arbitrary level of accuracy by limiting the in-between room propagations, while still accounting for infinitely many interactions within each room. This reduces the required computation time significantly, in particular for complex environments. The method is applicable to other complex environments provided the VSFG is sparse.

References

[1] T. Pedersen, G. Steinböck, and B. H. Fleury, "Modeling of reverberant radio channels using propagation graphs," *IEEE Trans. Antennas Propag.*, vol. 60, no. 12, pp. 5978–5988, Dec 2012.

[2] J. Chen, X. Yin, L. Tian, and M. D. Kim, "Millimeter-wave channel modeling based on a unified propagation graph theory," *IEEE Commun. Lett.*, vol. 21, no. 2, pp. 246–249, Feb 2017.

[3] W. Cheng, C. Tao, L. Liu, R. Sun, and T. Zhou, "Geometrical channel characterization for high speed railway environments using propagation graphs methods," in *Intern. Conf. on Adv. Comm Tech.*, Feb 2014, pp. 239–243.

[4] L. Tian, V. Degli-Esposti, E. M. Vitucci, X. Yin, F. Mani, and S. X. Lu, "Semi-deterministic modeling of diffuse scattering component based on propagation graph theory," in *IEEE PIMRC*, Sept 2014, pp. 155–160.

[5] T. Zhou, C. Tao, S. Salous, Z. Tan, L. Liu, and L. Tian, "Graph-based stochastic model for high-speed railway cutting scenarios," *IET Microwaves, Antennas Propagation*, vol. 9, no. 15, pp. 1691–1697, 2015.

[6] D. K. Ntaikos, A. C. Iossifides, and T. V. Yioultsis, "Enhanced graph-theoretic channel model for performance evaluation of MIMO antennas and millimeter wave communications," in *EuCAP*, May 2015, pp. 1–4.

[7] T. Pedersen, G. Steinböck, and B. H. Fleury, "Modeling of outdoor-to-indoor radio channels via propagation graphs," in *URSI General Assembly and Scientific Symposium*, Aug 2014, pp. 1–4.

[8] R. Adeogun and T. Pedersen, "Propagation graph based model for multipolarized wireless channels," in *IEEE WCNC*, April 2018.

[9] G. Steinböck, M. Gan, P. Meissner, E. Leitinger, K. Witrisal, T. Zemen, and T. Pedersen, "Hybrid model for reverberant indoor radio channels using rays and graphs," *IEEE Trans. Antennas Propag.*, vol. 64, no. 9, pp. 4036–4048, Sept 2016.

[10] L. Tian, V. Degli-Esposti, E. M. Vitucci, and X. Yin, "Semi-deterministic radio channel modeling based on graph theory and ray-tracing," *IEEE Trans. Antennas Propag.*, vol. 64, no. 6, pp. 2475–2486, June 2016.

[11] M. Gan, G. Steinböck, Z. Xu, T. Pedersen, and T. Zemen, "A hybrid ray and graph model for simulating vehicle-to-vehicle channels in tunnels," *IEEE Trans. Veh. Technol.*, vol. 67, no. 9, pp. 7955–7968, Sept 2018.

[12] Y. Miao, T. Pedersen, M. Gan, E. Vinogradov, and C. Oestges, "Reverberant room-to-room radio channel prediction by using rays and graphs," *IEEE Trans. Antennas Propag.*, vol. Early Access, 2018.

[13] R. Adeogun, T. Pedersen, and A. Bharti, "Transfer function computation for complex indoor channels using propagation graphs," *IEEE PIMRC*, Sept. 2018.